Persistent warmth across the Benguela upwelling system during the Pliocene epoch

Antoni Rosell-Melé[1,2]*, Alfredo Martínez-Garcia[3] and Erin L. McClymont[4†]

[1] *Institut de Ciència i Tecnologia Ambientals (ICTA) and Department of Geography, Universitat Autònoma de Barcelona, Bellaterra, Catalonia, Spain*

[2] *Institució Catalana de Recerca i Estudis Avançats (ICREA), Barcelona, Catalonia, Spain*

[3] *Geological Institute, ETH Zürich, Zürich, Switzerland*

[4] *School of Geography Politics and Sociology, Newcastle University, Newcastle upon Tyne, UK*

[†] *Present address: Department of Geography, Durham University, Durham, UK*

**Corresponding author. Tel.: +34 93 581 3583; Fax: +34 93 581 3331;*

antoni.rosell@uab.cat

ABSTRACT

A feature of Pliocene climate is the occurrence of "permanent El Niño-like" or "El Padre" conditions in the Pacific Ocean. From the analysis of sediment cores in the modern northern Benguela upwelling, we show that the mean oceanographic state off Southwest Africa during the warm Pliocene epoch was also analogous to that of a persistent Benguela "El Niño". At present these events occur when massive southward flows of warm and nutrient-poor waters extend along the coasts of Angola and Namibia, with dramatic effects on regional marine ecosystems and rainfall. We propose that the persistent warmth across

the Pliocene in the Benguela upwelling ended synchronously with the narrowing of the Indonesian seaway, and the early intensification of the Northern Hemisphere Glaciations around 3.0-3.5 Ma. The emergence of obliquity-related cycles in the Benguela sea surface temperatures (SST) after 3 Ma highlights the development of strengthened links to high latitude orbital forcing. The subsequent evolution of the Benguela upwelling system was characterized by the progressive intensification of the meridional SST gradients, and the emergence of the 100 ky cycle, until the modern mean conditions were set at the end of the Mid Pleistocene transition, around 0.6 Ma. These findings support the notion that the interplay of changes in the depth of the global thermocline, atmospheric circulation and tectonics preconditioned the climate system for the end of the warm Pliocene epoch and the subsequent intensification of the ice ages.

Highlights

1. Persistent Benguela “El Niño” during the warm Pliocene epoch
2. Ended synchronously with the narrowing of the Indonesian seaway
3. Intensification of Benguela meridional temperature gradients went in parallel with Subantarctic dust deposition
4. Plio-Pleistocene orbital variability analogous to that in Eastern Equatorial Pacific

Abbreviations:

Angola-Benguela Frontal Zone (ABFZ); sea surface temperatures (SST); Ocean Drilling Program (ODP); Alkenone mass accumulation rates (MAR); Mid Pleistocene Transition (MPT); Indonesian Throughflow (ITF)

Keywords

Plio-Pleistocene transition; Benguela upwelling; sea surface temperature; export productivity; "El Niño"-like; Indonesian seaway; Northern Hemisphere Glaciation; wavelet analysis; orbital variability

1. Introduction

The Benguela upwelling system (BUS) forms part of one of the world's major eastern boundary current systems. The Angola Current and the northern BUS meet at about 15 ºS (with an annual variability of 2-3º latitude) where their boundaries are defined by the Angola-Benguela Frontal Zone, or ABFZ (Meeuwis and Lutjeharms, 1990) (Fig. 1). Southward protrusions of warm Angola Current water sporadically extend along the African coast as far as 25 ºS (Shannon et al., 1986). They are marked by a reduction in upwelling, and associated with anomalous increases in precipitation, disruptions to fish, bird and mammal migrations and adverse impacts on fish populations (Rouault et al., 2003). They have been called Benguela "El Niño" events (Shannon et al., 1986) because of the similarities with sea surface fluctuations along the South American coast associated with the El Niño/Southern Oscillation, but it is not clear which processes drive the Benguela events. Some authors argue that the origin of the Benguela "El Niño" is remotely forced by zonal wind stress anomalies in the equatorial Atlantic, triggering Kelvin waves that propagate along the equator and subsequently along the southwest African coast where they induce downwelling anomalies (Florenchie et al., 2003; Shannon et al., 1986). An alternative proposition is that sea surface temperatures (SSTs) along the southwest African coast respond to a basin scale weakening of the South Atlantic subtropical anticyclone which induces a weakening of the southeasterly trades (Lübbecke et al., 2010; Richter et al., 2010).

Determining the timing and magnitude of changes in the BUS across the Plio-Pleistocene is important because model experiments suggest that the appearance of cold

waters in subtropical and tropical upwelling regions may have had a significant effect in ending the Pliocene global warmth (Barreiro et al., 2006; Philander and Fedorov, 2003). The transition between the Pliocene and Pleistocene epochs was marked by the development of extensive bipolar glaciations (Ravelo et al., 2004). The subsequent strengthening of the meridional and zonal temperature gradients in association with increasing ice volume resulted in an equatorward expansion of the polar oceans, and an intensification and equatorward contraction of the atmospheric convective cells (Brierley et al., 2009; Etourneau et al., 2010; Fedorov et al., 2013; Martinez-Garcia et al., 2010). These changes in atmospheric circulation should have impacted the variability of the major eastern boundary currents of the sub-tropical gyres driven by the easterly trade winds and, particularly, in the wind-driven upwelling system of Benguela where the distinct coastal regime is greatly influenced by the South Atlantic subtropical anticyclone.

Variability in upwelling intensity in response to both glacial-interglacial oscillations and over longer timescales have been identified by alternating horizons of organic carbon- and carbonate-rich sediments in the BUS since the initiation of the upwelling during the mid-Miocene (Bruchert et al., 2000; Diester-Haass et al., 1986; Diester-Haass et al., 2002; Etourneau et al., 2009; Giraudeau et al., 2000; Giraudeau et al., 2002; Marlow et al., 2000; Meyers, 2001; Siesser, 1980; Summerhayes et al., 1995). The Pliocene-Pleistocene transition resulted in upwelling intensification in the central and Northern Benguela region (e.g. Christensen et al., 2002; Marlow et al., 2000), which has also been observed in other eastern boundary current systems (Dekens et al., 2007; Herbert and Schuffert, 1998). A comparison of organic carbon and carbonate accumulation rates off southwestern Africa also identified the development of the modern division between a northern perennial

upwelling region, and a more seasonal upwelling signature to the south by ca. 2 Ma (Giraudeau et al., 2002). The late Pliocene sediments from the BUS are also marked by the 'Matuyama Diatom Maximum' (MDM), a period of extensive peak opal deposition that spans from 20ºS and 30ºS, and that occurred synchronously with biogenic opal maxima in upwelling systems in other parts of the world such as off California and Mauritania (Janecek, 2000; Tiedemann, 1991). During the MDM, SSTs in Benguela and other upwelling systems of the world cooled synchronously (Dekens et al., 2007; Etourneau et al., 2009; Herbert and Schuffert, 1998; Liu et al., 2008; Marlow et al., 2000). However, the high opal contents characteristic of the MDM are not mirrored by an increase in the accumulation of organic carbon (Berger et al., 2002; Etourneau et al., 2012; Lange et al., 1999; Marlow et al., 2000). The MDM is interpreted to have formed beneath the frontal boundary between the cold upwelled water and the offshore warmer South Atlantic surface water during episodes of equatorward excursions of polar waters into the BUS (Berger et al., 2002; Lange et al., 1999; Marlow et al., 2000). After the MDM, there is a general decrease in opal and diatom deposition and a change in the composition of the diatom flora, but the increase in organic matter and upwelling species points to increased importance of coastal upwelling toward the present (Berger et al., 2002; Etourneau et al., 2009; Marlow et al., 2000).

To investigate further the processes that drove changes in the BUS across the Pliocene-Pleistocene, we evaluate to which extent some of the transitions that occurred at orbital and longer timescales were linked to conditions in the Southern Ocean. We have focused our discussion especially in the Pliocene, an epoch when the South Atlantic atmospheric convective cells extended further poleward than today, greatly affecting wind

intensity and global precipitation patterns (Barreiro et al., 2006; Brierley et al., 2009; Martinez-Garcia et al., 2011; Martinez-Garcia et al., 2010). We have tested whether Pliocene mean climatic conditions resulted in a climatic state off south western Africa analogous to that of a persistent Benguela "El Niño". We note that we have investigated a steady-state change (change in the mean state, and the occurrence of Benguela "El Niño-like" conditions), and not a change in interannual variability as correspond to modern Benguela "El Niño" events.

2. Study Sites

The BUS runs parallel to the coastline of southern Africa (Fig. 1). The upwelling is driven by the combination of the offshore divergence as the Benguela Current and eastern limb of the South Atlantic gyre flow equatorwards, and the longshore winds generated by low pressure over the Kalahari desert (Dowsett and Willard, 1996; Hay and Brock, 1992). The sources of the Benguela Current waters are diverse, including Indian and South Atlantic subtropical thermocline water; saline, low-oxygen tropical Atlantic water; and cooler, fresher Subantarctic Mode Water (SAMW) (Garzoli and Gordon, 1996). The Indian Ocean water can amount to 25% of the total and is injected into the Benguela Current through the Aghulas retroflection eddy and filament process (Garzoli et al., 1996). At present, when the Benguela Current increases in strength it brings in more subtropical water (Garzoli et al., 1996). The upwelling also brings to the surface cold and nutrient-rich waters from the subduction zones of surface water at the Subtropical-Subantarctic Front (Lutjeharms and Valentine, 1987). The high nutrient content of the upwelling waters fuels

high levels of production in the surface ocean and high rates of organic carbon sequestration to the sediments below (Mollenhauer et al., 2004; Schneider and Müller, 1995).

The upwelling is not a uniform process in the present-day BUS. In the northern BUS, the upwelling is perennial and may extend well offshore in filaments of cold and nutrient-rich waters that create year-round high productivity (Lutjeharms and Stockton, 1987). The perennial upwelling and high nutrient contents of the upwelling waters drives high levels of production, which can be traced in surface sediments by high levels of organic carbon (up to 9% dry weight, Mollenhauer et al., 2004). This contrasts with the seasonal upwelling system and lower nutrient contents that characterize the southern BUS, identified by the lower organic carbon contents found in surface sediments relative to those in the north (Rogers and Bremner, 1991). SSTs in the southern BUS also reflect the balance between the relative inputs of Indian Ocean (via the Agulhas retroflection) and cool Southern Ocean waters from the Antarctic Circumpolar Current (ACC) system to the south. The relative importance of these inputs has varied through time, particularly during glacial-interglacial oscillations, with northward migrations of the ACC during glacials argued to have restricted or blocked the exchange of Indian Ocean waters with the south-east Atlantic (e.g. McClymont et al., 2005; McIntyre et al., 1989; Peeters et al., 2004).

We have compared the evolution of SST and marine export productivity in three sites currently south of the ABFZ, drilled during Ocean Drilling Program (ODP) Leg 175 (Fig. 1). Sites 1081 (19°37´S, 11°19´E, 794 m water depth) and 1082 (21°5′S, 11°49′E, 1280 m water depth) were drilled under the zone of modern perennial upwelling and below the northward flowing Benguela Current (Wefer et al., 1998). Site 1084 (25°31´S, 13°02´E,

1992 m water depth) is in close proximity to the highly active and central (Lüderitz) upwelling cell in the Northern Cape Basin (Wefer et al., 1998) and in the centre of the BUS. SSTs are quantified using the alkenone unsaturation index U^{K}_{37}' (Brassell et al., 1986). Export productivity is inferred using alkenone biomarker accumulation rates which *sensu stricto* only reflects Haptophyte algae export productivity. Alkenone mass accumulation rates (MAR) have been shown, however, to relate to export productivity fluxes (Bolton et al., 2011), as they display a good agreement with total chlorophyll MAR in the sites studied over timescales >100 ky (Marlow, 2001). Our new data from ODP 1081 and ODP 1084 is combined with previously published results from ODP 1082 (Etourneau et al., 2009).

3. Methods

3.1. Alkenone analysis.

Sediment samples were freeze-dried, homogenised, and solvent extracted by sonication. Solvent extracts from Site 1084 were fractionated into apolar and polar fractions with column chromatography using silica gel as adsorbent and elution solvents consisting of (F1) dichloromethane:hexane (1:1, v:v) and (F2) dichloromethane:methanol (1:1, v:v). Alkenones (F1) were identified and quantified with a gas chromatograph fitted with a split/splitless injector (300°C) and a flame ionization detector (330°C), using hexatriacontane as internal standard. Separation of the target compounds was achieved with an Agilent J&W HP-1 capillary column (60 m, 0.25 mm internal diameter, 0.25 μm film thickness) and a capillary precolumn (5 m, 0.25 mm internal diameter, 0.25 μm film

thickness), and helium as the carrier gas (1.5 ml min^{-1}). The oven temperature program was 45ºC to 245ºC at 20ºC/min and 245ºC to 305ºC at 10ºC/min. Total solvent extracts from Site 1081 were derivatized with bis-(trimethylsilyl) trifluoroacetamide (BSTFA, Fluka, >98%) in DCM (100µl of each at 70ºC for 2 hr in N_2 purged vials) immediately prior to analysis. Analysis was made by gas chromatography with automated split/splitless injection (held at 280ºC) and flame ionisation detection (GC-FID, Fisons 8000 Series with AS 800 auto-sampler). Separation was performed using an HP1 fused silica capillary column (30 m x 0.32 mm internal diameter). Hydrogen was used as carrier gas (0.6 kg/cm^2) and the oven temperature program was 45ºC to 245ºC at 20ºC/min and 245ºC to 305ºC at 10ºC/min.

3.2. Age models.

For a better comparison of the evolution of the different SST records of the BUS through the Pliocene-Pleistocene, in this study the age models of ODP sites 1081 and 1084 are generated by aligning the new SST estimates to the existing paleotemperature estimates from the nearby site ODP 1082 (Etourneau et al., 2009) using the software Analyseries (Paillard et al., 1996), which in turn is based on the alignment of a benthic/planktonic $\delta^{18}O$ record and alkenone SSTs to the LR04 oxygen isotope stack over the last 3.5 Ma (Etourneau et al., 2009) (Figs. 2 and 3). In the older part of the records, the magnetostratigraphy and calcareous nannofossil biostratigraphy ages (Wefer et al., 1998) are used. In Fig. 3 we show a comparison of the new age model estimates obtained by SST alignment and the existing magnetostratigraphy and biostratigraphy chronologies (Wefer et

al., 1998). The sampling resolution of the records is suborbital from 0 to 1.5 Ma for Site 1081, and from 0 to 2.2 Ma for Site 1084.

4. Results

The new data presented here extend the mid-Pleistocene alkenone data sets from Site 1081 (Durham et al., 2001) back to 5 Ma, significantly increase the resolution of the previously published Pliocene-Pleistocene data set from Site 1084 (Marlow et al., 2000), and are presented using revised age models that allow a more detailed comparison of the variability of the different records through time (data are available from the Pangaea database at http://www.pangaea.de/). The precision of the alkenone paleothermometer is supported by the remarkable close agreement of the absolute SST reconstructions from our northernmost Site 1081 and published data from the nearby Site 1082 (Etourneau et al., 2009) (Figs. 2 and 4), and the replication of the modern SST gradient across northern Benguela by the core top SST estimates (Figs.1 and 2).

A conspicuous feature in all of the SST records is the continuous cooling across the Pliocene-Pleistocene, from 5-3.5 Ma to the end of the Mid Pleistocene Transition (MPT) ca 0.6 Ma (Fig. 4). Site 1081 from the northernmost upwelling region depicts an overall cooling range of ca. 9°C whereas a 12.5°C range is observed in Site 1084, even though the overall trends and patterns of the glacial/interglacial variability are remarkably similar (Fig. 2). Notably, prior to around 3.5 Ma the SST gradient between both sites was at zero, in contrast to the modern gradient of around 4°C (Figs. 1 and 5), and export productivity was low in both sites. The onset of the gradual increase in the SST gradient from around 3.5

Ma was driven by a larger mean increase in the rate of cooling in Site 1084 relative to 1081 and 1082. Despite falling SSTs and an increasing SST gradient since 3.5 Ma, export productivity did not increase above background levels until the period ca. 2.4–2.0 Ma. At Site 1084, export productivity maxima occurred prior to the MPT, from ca. 1.5 Ma, when there was an increase in the SST gradient between sites 1081 and 1084 (Fig. 4) and an increase in the rate of cooling in both records (Fig. 4). However, Site 1081 maxima in export production increase later, in association with the end of the MPT from 0.6 Ma (Fig. 4). The modern situation was thus reached after the MPT ca. 0.6 Ma when export productivity at both sites was high and the SST gradient was comparable to the modern (Fig. 4).

5. Discussion

5.1. Pliocene-Pleistocene climatic transitions

The major transitions over the Pliocene-Pleistocene in the BUS mark an overall strengthening of upwelling, which has been postulated to be related to a change in atmospheric circulation via the Southeast Atlantic high-pressure cell, tied to a cooling in the Southern Ocean, and the equatorward movement of the Southern Ocean fronts (Etourneau et al., 2009; Giraudeau et al., 2002). In fact, we do observe that the trends in the SST gradients between the central and northern Benguela sites occurred in very close correspondence with the long term variability in dust deposition in the Subantarctic Atlantic (Martinez-Garcia et al., 2011) (Fig. 4D). The parallel change in the gradient and cooling in SSTs in the BUS with the increase in atmospheric dust transport after 3.5-3.2 Ma in the

253 Southern Ocean further points to the link between BUS conditions and the intensification of
254 atmospheric circulation in the South Atlantic across the Pliocene-Pleistocene (Fig. 4D).

255 The SST cooling trend observed in the BUS after the late Pliocene and the onset of
256 the Northern Hemisphere Glaciation (NHG) and the MDM may have had a variety of
257 causes, related to global and regional processes (Berger et al., 2002; Lange et al., 1999;
258 Marlow et al., 2000; Martinez-Garcia et al., 2010). Etourneau et al. (2009) discussed how
259 lower SSTs during the MDM at the BUS (Site 1082) was related to a change in the
260 thermocline depth and outcropping of cold AAIW which transported silica rich Southern
261 Ocean waters equatorwards and to the BUS (Cortese et al., 2004; Hillenbrand and Cortese,
262 2006; Marlow et al., 2000; Robinson and Meyers, 2002). The high silicic acid contents in
263 the AAIW would have resulted from the enhanced stratification and decrease in opal
264 production in the Antarctic Ocean (Sigman et al., 2004). Lawrence et al. (2006) also
265 proposed that the unused nutrients at high latitudes were transported by upwelling source
266 waters, primarily from the Southern Ocean, and also led to a marked rise in productivity in
267 the Eastern Equatorial Pacific after 3 Ma and associated with the intensification of the
268 NHG.

269 Based partly on changes in diatom flora in the central BUS (Garzoli and Gordon,
270 1996; Marlow et al., 2000), export productivity and $\delta^{15}N$ sediment data, the interval at 2.4-
271 2.0 Ma has been interpreted to mark a switch in the source of the upwelled waters from the
272 AAIW to the SAMW, and the beginning of the modern BUS seasonal pattern as a result of
273 a strengthening in the trade winds (Etourneau et al., 2009). However, some of these
274 findings are partly based on the comparison of records between site 1082 and the

275 previously published and lower resolution data from site 1084. Here, we show that with an
276 increase in the sampling resolution of Site 1084 we could synchronize the age models of
277 both sites using their SST records at a orbital-scale resolution, and together with the data
278 from Site 1081, it is apparent that a significant increase in alkenone export production did
279 occur from 2.4-2.0 Ma (Fig. 4C), but with no significant change in the meridional SST
280 gradient between the central and northern BUS (Fig. 4D). During this time interval frontal
281 systems developed in the Southern Ocean (Liu et al., 2008), together with an increase in
282 Southern Ocean siliceous productivity (Cortese et al., 2004), which probably restricted the
283 subsurface water transfer to low latitude regions like the BUS and reduced the nutrient
284 content in the source water. This likely led to the demise of the MDM and diatom
285 production in upwelling areas (Etourneau et al., 2012; Marlow et al., 2000).

286 The meridional SST gradient between the northern and central BUS started
287 increasing at 1.5 Ma (Fig. 4D), with a concomitant increase in export productivity. The
288 modern gradient in SST between the northern and central upwelling sites was reached at
289 0.6 Ma, together with the highest values of export productivity (Figs. 2C and 2D). This
290 change after the end of the MPT would reflect formation of the modern Southern Ocean
291 fronts and the strengthening of the atmospheric circulation and trade winds as observed by
292 a marked increase in dust in the Subantarctic Atlantic (Martinez-Garcia et al., 2011), the
293 formation of Subantarctic waters and deeper equatorward circulation of AAIW (Etourneau
294 et al., 2009). Thus, the Pleistocene increase in the global meridional temperature gradients,
295 enhanced atmospheric convection and equatorward expansion of the polar margins
296 (Martinez-Garcia et al., 2010), and a shallower global thermocline (Philander and Fedorov,
297 2003) led to the gradual equatorward migration and intensification of the coastal Benguela

298 upwelling until it reached the modern oceanographic configuration, typical of a colder
299 mean climate than in the Pliocene.
300
301 *5.2. Variability in orbital frequencies*
302 To investigate further the interplay between climate long-term trends and orbital
303 scale variability in the BUS we have undertaken a wavelet spectral analysis on the alkenone
304 SST and MAR records from Site 1084 (this study) and published data from Site 1082
305 (Etourneau et al., 2009). On the sections in which they overlap, the spectra in both sites are
306 very similar (Fig. 6). SST variability associated to obliquity (41 ky period) intensifies after
307 3 Ma and becomes significant above red noise around 2.7 Ma (Figs. 6 and 7). Variability at
308 the precession frequency, however, is weak throughout the record. The 100 ky cycle
309 emerges and dominates after ca. 0.6 Ma, the end of the MPT, both in sites 1082 and 1084.
310 This pattern has not previously been described for the BUS, but it is remarkably similar to
311 what has been shown for the Eastern Equatorial Pacific (Lawrence et al., 2006), and
312 suggests that high-latitude processes start to drive low-latitude climate variability on the
313 obliquity band (41-ky) after 3 Ma (Fig. 7).
314 However, it is not straightforward to investigate the links between the presence of a
315 41 ky period with high latitude climate during the late Pliocene and early Pleistocene, due
316 to the limited number of records presently available (especially in the Southern Ocean)
317 which also have the adequate resolution and chronology. The emergence of strong 41 ky
318 periodicity does not occur in the only available Southern Ocean SST record (ODP Site
319 1090) until after 1.8 Ma (Martinez-Garcia et al., 2010). However, this may be due to the

poleward expanded tropical warm pool at that time which may have decreased the sensitivity of the record to higher latitude insolation forcing prior to 1.8 Ma (Martinez-Garcia et al., 2010). However, both the global $\delta^{18}O$ record (Lisiecki and Raymo, 2005) and the available North Atlantic SST records (ODP Site 982) show evidence of strong obliquity cycles during the late Pliocene and early Pleistocene (Lawrence et al., 2009) in the high latitudes of the Northern Hemisphere (Fig. 7).

The presence of the MDM, as discussed here previously, does show support for changing diatom productivity linked to longer-term changes in Southern Ocean circulation and nutrient supply to the Benguela system (e.g. Etourneau et al., 2009). But those same data sets have not been presented with time-series analysis to determine what may pace any shorter-term variations in productivity, and how that might relate to the pacing of the SST cycles identified here.

The emergence of the 41 ky cycles in the Benguela data sets occurs as higher $\delta^{30}Si$ values in ODP 1082 are interpreted to reflect a longer term trend towards increased silicate utilization partly in response to enhanced silicate supply from the Southern Ocean (Etourneau et al., 2012). However, whether upwelling intensity and/or Benguela SSTs were also determined by Southern Ocean circulation at the 41 ky period is not clear given the low resolution of the $\delta^{30}Si$ data, and an absence of 41 ka cycles in SST at ODP 1090 (Martinez-Garcia et al., 2010). The absence of significant precession cycles in our time time series analysis would also indicate that low latitude processes at orbital scales play a marginal role in driving variations in SST at the BUS, especially prior to the MPT, which

341 has also been observed in the eastern equatorial Pacific (Lawrence et al., 2006; Liu and
342 Herbert, 2004).

343 As argued in the previous section, the influence of high latitude processes at the
344 BUS could have occurred through a shoaling of the thermocline, identified by a cooling in
345 SST, and the subsurface advection of subpolar/polar waters that in the Benguela region
346 marked the onset of the MDM (Berger et al., 2002; Lange et al., 1999; Marlow et al., 2000).
347 A further increase in the intensity of the 41 ky obliquity band in sites 1082 and 1084
348 happens at 1.5 Ma (Figs 3B and S3B), coincidental with an increase in dust/atmospheric
349 circulation and cooling in the Subantarctic (Fig. 4D) (Martinez-Garcia et al., 2011;
350 Martinez-Garcia et al., 2010), which coincides with an increase in alkenone MAR in
351 northern (Etourneau et al., 2009) and central Benguela (Fig. 4C). This export production
352 increase could denote a further shoaling of the thermocline and suggests the influence of
353 Southern Ocean waters in the BUS, which after 1.5 Ma may have originated in the
354 Subantarctic as SAMW (Etourneau et al., 2009).

355 The spectra of the alkenones MAR is less clear. Significant precession and obliquity
356 cycles occur in different parts of the record and there is a strong 400ky cycle, probably
357 related to the eccentricity modulation of precession, suggesting an important role of low
358 latitude climate in controlling productivity changes (Fig. 6). Surprisingly, the 100 ky cycle
359 in the productivity records is significant during the MPT but not afterwards.

360

361 *5.3. Pliocene Benguela "El Niño"-like mean state*

362 The lack of a SST gradient between the northern and central sites of the BUS
363 together with their low export productivity fluxes and relatively warm SSTs prior to 3.5 Ma
364 indicate that the ABFZ was displaced south of Site 1084 (Fig. 4), and hence that the mean
365 oceanographic conditions in the Southeast Atlantic at timescales >100ky were analogous to
366 that of a persistent Benguela "El Niño"-like scenario. This would imply that warm Angola
367 Current water extended along the African margin south of the location of Site 1084
368 (25°31'N).

369 Low Subantarctic dust deposition in the Pliocene has been interpreted as a
370 consequence of weak atmospheric convective cells that extended further poleward, and
371 probably gave rise to a weakening of the South Atlantic subtropical anticyclone (Barreiro et
372 al., 2006; Brierley et al., 2009; Martinez-Garcia et al., 2011; Martinez-Garcia et al., 2010).
373 This scenario is coherent with the occurrence of weaker southeasterly trades and reduced
374 upwelling (and low organic carbon accumulation in bottom sediments) as is observed to
375 occur during modern Benguela "El Niño" events (Lübbecke et al., 2010; Richter et al.,
376 2010). The analogy with modern conditions of Benguela "El Niño"-like patterns also
377 presupposes the occurrence of increased precipitation onshore in South western Africa
378 during the Pliocene, which is also shown by models (e.g. Brierley et al., 2009; Haywood et
379 al., 2002). This is corroborated by evidence from a pollen record in Site 1082, which was
380 interpreted to reflect a shift from a few areas with desert/semidesert vegetation prior to 3
381 Ma, to a gradual increase in aridification towards the present (Dupont, 2006; Dupont et al.,
382 2005).

383 The initial onset in the meridional SST gradient in the northern Benguela upwelling
384 around 3.5 Ma coincided with the early onset of the intensification of the NHG from 3.6

385 Ma to 2.4 Ma, whose root cause has been ascribed to a long-term tectonic forcing such as
386 closing or narrowing of ocean gateways, or mountain building (Mudelsee and Raymo,
387 2005). Some authors have hypothesized that the increase in SSTs in Benguela during the
388 Pliocene is related to the closure of the Central American Seaway or CAS (Prange and
389 Schulz, 2004). Closure of the CAS could have resulted in changes in the Atlantic
390 meridional overturning circulation (AMOC), leading to a general cooling of the southern
391 hemisphere, and might have played a secondary role in the initiation of the NHG (Lunt et
392 al., 2008), although a significant role for the CAS in global climate change has also been
393 questioned (Molnar, 2008). However, a change in the AMOC initiated by the progressive
394 closure of the CAS took place between 4.8 and 4.0 million years ago, beyond the time span
395 over which all our records overlap.
396 The timing of the cooling of the surface and subsurface eastern Indian Ocean at 3.5
397 Ma (inferred from Mg/Ca ratios of planktonic foraminifera in sites DSDP 214 and ODP
398 763; Figs. 1 and 7C) (Karas et al., 2009; Karas et al., 2011), which is postulated to be an
399 outcome from the tectonically-driven reduction of the Indonesian Throughflow (ITF, ca.
400 2.95 - 3.5 Ma) (Cane and Molnar, 2001), is coeval with the end of the permanent Benguela
401 "El Niño"-like state off Southwest Africa, a cooling of the surface Subantarctic Atlantic
402 (Martinez-Garcia et al., 2010) (Fig. 5), and a cooling of SSTs in the North Atlantic
403 (Lawrence et al., 2009) . Our findings lend support to the view that the reduction of the ITF
404 diminished heat transport from the Indian Ocean polewards and to the South Atlantic
405 (Karas et al., 2011). We hypothesize that this may have led to a series of climatic changes
406 in the Southern Ocean (i.e. poleward movement of frontal zones) that preconditioned the
407 climate system for the intensification of the NHG and its impact on low latitude climate

(i.e. through changes in the depth of the thermocline and temperature and nutrient contents of source waters). We note that if the ITF changes are implicated in intensifying the NHG, which subsequently led to equatorward contraction of atmospheric circulation cells and therefore the increased SST gradient observed beginning 3.5 Ma, then this implies a somewhat earlier start to intensified NHG glaciation than is commonly accepted.

6. Conclusion

Our study indicates that the modern structure of the BUS characterized by intense upwelling, cold SST, and high biological productivity, is not stable over long time scales. Although our data do not allow us to resolve the frequencies characteristics of modern "El Niño" events, they provide strong evidence for a fundamental change in the mean state of the BUS during the Pliocene epoch that resulted in regional climatic conditions analogous to those of a persistent Benguela "El Niño". The Benguela and Pacific "El Niños" may respond to different forcing mechanisms in the modern ocean, but the two systems appear to be particularly sensitive to the changes in the mean state of the climate system that characterize the warm Pliocene epoch, suggesting that both regions may be susceptible to profound changes under prolonged anthropogenic forcing of climate.

In turn, these trends are associated by the emergence of different orbital signals, which reflect an evolving response of the Benguela system to high-latitude processes as the mean state of the region changes. The described sequence of changes in the BUS across the Pliocene-Pleistocene can be interpreted as the result of the interplay of processes occurring at regional and global scales, to which the Benguela region appears to be particularly sensitive. Thus, the Benguela records reflect the ongoing Cenozoic global cooling trend,

which probably led to a gradual global shoaling of the thermocline (Philander and Fedorov, 2003), and a progressive increase in the response of low-latitude climate to high latitude orbital forcing (Lawrence et al., 2006). Our study would further suggest the influence of Southern Ocean oceanographic changes on the evolution of the BUS and other major upwelling systems.

Acknowledgements

This research used samples and/or data provided by the Ocean Drilling Program (ODP). ODP is sponsored by the U.S. National Science Foundation (NSF) and participating countries under the management of Joint Oceanographic Institutions. A. Sansón, E.L Durham, J. Marlow and P. Bracke are acknowledged for analyzing some of the records and early discussions. The late Johann Lutjeharms, Sam Jaccard and Gerald Haug are acknowledged for their feedback on the ideas discussed in the manuscript. Financial support for this research was provided by a Marie Curie-IOF fellowship (235626) to ARM, and a grant from the Spanish MICINN (CGL2008-03288-E).

References

Barreiro, M., Philander, G., Pacanowski, R., Fedorov, A., 2006. Simulations of warm tropical conditions with application to middle Pliocene atmospheres. Clim. Dyn. 26, 349-365.

Berger, W.H., Lange, C.B., Pérez, M.E., 2002. The early Matuyama Diatom Maximum off SW Africa: a conceptual model. Marine Geology 180, 105-116.

Bolton, C.T., Lawrence, K.T., Gibbs, S.J., Wilson, P.A., Herbert, T.D., 2011. Biotic and geochemical evidence for a global latitudinal shift in ocean biogeochemistry and export productivity during the late Pliocene. Earth Planet. Sci. Lett. 308, 200-210.

Brassell, S.C., Eglinton, G., Marlowe, I.T., Pflaumann, U., Sarnthein, M., 1986. Molecular stratigraphy: a new tool for climatic assessment. Nature 320, 129-133.

Brierley, C.M., Fedorov, A.V., Liu, Z., Herbert, T.D., Lawrence, K.T., LaRiviere, J.P., 2009. Greatly expanded tropical warm pool and weakened hadley circulation in the early pliocene. Science 323, 1714-1718.

Bruchert, V., Elena Perez, M., Lange, C.B., 2000. Coupled primary production, benthic foraminiferal assemblage and sulfur diagenesis in organic-rich sediments of the Benguela upwelling system. Marine Geology 163, 27-40.

Cane, M.A., Molnar, P., 2001. Closing of the Indonesian seaway as a precursor to east African aridification around 3-4 million years ago. Nature 411, 157-162.

466 Christensen, B.A., Kalbas, J.L., Maslin, M.A., Murray, R.W., 2002. Paleoclimate changes
467 in southern Africa during the intensification of Northern Hemisphere glaciation: evidence
468 from ODP Leg 175 Site 1085. Marine Geology 180, 117-131.

469 Cortese, G., Gersonde, R., Hillenbrand, C.D., Kuhn, G., 2004. Opal sedimentation shifts in
470 the World Ocean over the last 15 Myr. Earth Planet. Sci. Lett. 224, 509-527.

471 Dekens, P.S., Ravelo, A.C., McCarthy, M.D., 2007. Warm upwelling regions in the
472 Pliocene warm period. Paleoceanography 22.

473 Diester-Haass, L., Meyers, P.A., Rothe, P., 1986. Light-dark cycles in opal-rich sediments
474 near the Plio-Pleistocene boundary, DSDP Site 532, Walvis Ridge Continental Terrace.
475 Marine Geology 73, 1-23.

476 Diester-Haass, L., Meyers, P.A., Vidal, L., 2002. The late Miocene onset of high
477 productivity in the Benguela Current upwelling system as part of a global pattern. Marine
478 Geology 180, 87-103.

479 Dowsett, H., Willard, D., 1996. Southeast Atlantic marine and terrestrial response to middle
480 Pliocene climate change. Marine Micropaleontology 27, 181-193.

481 Dupont, L.M., 2006. Late Pliocene vegetation and climate in Namibia (southern Africa)
482 derived from palynology of ODP Site 1082. Geochem Geophy Geosy 7.

483 Dupont, L.M., Donner, B., Vidal, L., Perez, E.M., Wefer, G., 2005. Linking desert
484 evolution and coastal upwelling: Pliocene climate change in Namibia. Geology 33, 461-
485 464.

486 Durham, E.L., Maslin, M.A., Platzman, E., Rosell-Melé, A., Marlow, J.R., Leng, M.,
487 Lowry, D., Burns, S.J., and the ODP Leg 175 Shipboard Scientific Party, 2001.
488 Reconstructing the climatic history of the western coast of Africa over the past 1.5 m.y.: a
489 comparison of proxy records from the Congo Basin and the Walvis Ridge and the search
490 for the Mid-Pleistocene Revolution, in: Wefer, G., Berger, W.H., Richter, C. (Eds.),
491 Proceedings of the Ocean Drilling Program, Scientific Results, pp. 1-46 [Online].

492 Etourneau, J., Ehlert, C., Frank, M., Martinez, P., Schneider, R., 2012. Contribution of
493 changes in opal productivity and nutrient distribution in the coastal upwelling systems to
494 Late Pliocene/Early Pleistocene climate cooling. Clim. Past 8, 1435-1445.

495 Etourneau, J., Martinez, P., Blanz, T., Schneider, R., 2009. Pliocene-Pleistocene variability
496 of upwelling activity, productivity, and nutrient cycling in the Benguela region. Geology
497 37, 871-874.

498 Etourneau, J., Schneider, R., Blanz, T., Martinez, P., 2010. Intensification of the Walker
499 and Hadley atmospheric circulations during the Pliocene-Pleistocene climate transition.
500 Earth Planet. Sci. Lett. 297, 103-110.

501 Fedorov, A.V., Brierley, C.M., Lawrence, K.T., Liu, Z., Dekens, P.S., Ravelo, A.C., 2013.
502 Patterns and mechanisms of early Pliocene warmth. Nature 496, 43-49.

503 Florenchie, P., Lutjeharms, J.R.E., Reason, C.J.C., Masson, S., Rouault, M., 2003. The
504 source of Benguela Ninos in the South Atlantic Ocean. Geophys. Res. Lett. 30, 12.11.

505 Garzoli, S.L., Gordon, A.L., 1996. Origins and variability of the Benguela Current. J.
506 Geophys. Res.-Oceans 101, 897-906.

507 Garzoli, S.L., Gordon, A.L., Kamenkovich, V., Pillsbury, D., DuncombeRae, C., 1996.
508 Variability and sources of the southeastern Atlantic circulation. J. Mar. Res. 54, 1039-1071.

509 Giraudeau, J., Bailey, G.W., Pujol, C., 2000. A high-resolution time-series analyses of
510 particle fluxes in the Northern Benguela coastal upwelling system: carbonate record of
511 changes in biogenic production and particle transfer processes. Deep-Sea Research II 47,
512 1999-2028.

513 Giraudeau, J., Meyers, P.A., Christensen, B.A., 2002. Accumulation of organic and
514 inorganic carbon in Pliocene-Pleistocene sediments along the SW African margin. Marine
515 Geology 180, 49-69.

516 Grinsted, A., Moore, J.C., Jevrejeva, S., 2004. Application of the cross wavelet transform
517 and wavelet coherence to geophysical time series. Nonlin. Processes Geophys. 11, 561-566.

518 Hay, W.H., Brock, J.C., 1992. Temporal variation in intensity of upwelling off southwest
519 Africa, in: Summerhayes, C.P., Prell, W.L., Emeis, K.-C. (Eds.), Upwelling Systems:
520 Evolution Since the Early Miocene. Geological Society Special Publication No 64, pp. 463-
521 497.

522 Haywood, A.M., Valdes, P.J., Francis, J.E., Sellwood, B.W., 2002. Global middle Pliocene
523 biome reconstruction: A data/model synthesis. Geochemistry, Geophysics, Geosystems 3,
524 1072.

525 Herbert, T.D., Schuffert, J.D., 1998. 2. Alkenone unsaturation estimates of Late Miocene
526 through Late Pliocene sea -surface temperatures at site 958, in: Firth, J.V. (Ed.),
527 Proceedings of the Ocean Drilling Program, Scientific Results, Vol. 159T, pp. 17-21.

528 Hillenbrand, C.D., Cortese, G., 2006. Polar stratification: A critical view from the Southern
529 Ocean. Palaeogeogr. Palaeoclimatol. Palaeoecol. 242, 240-252.

530 Janecek, T.R., 2000. Data report: Late neogene biogenic opal data Leg 167 sites on the
531 California margin, Proc. Ocean Drill. Progr.Sci. Res. 167, Ocean Drill. Progr. College
532 Station, Texas.

533 Karas, C., Nürnberg, D., Gupta, A.K., Tiedemann, R., Mohan, K., Bickert, T., 2009. Mid-
534 Pliocene climate change amplified by a switch in Indonesian subsurface throughflow.
535 Nature Geoscience 2, 434-438.

536 Karas, C., Nürnberg, D., Tiedemann, R., Garbe-Schönberg, D., 2011. Pliocene Indonesian
537 Throughflow and Leeuwin Current dynamics: Implications for Indian Ocean polar heat
538 flux. Paleoceanography 26, PA2217.

539 Lange, C.B., Berger, W.H., Lin, H.L., Wefer, G., Shipboard Sci Party, L., 1999. The early
540 Matuyama Diatom Maximum off SW Africa, Benguela Current System (ODP Leg 175).
541 Marine Geology 161, 93-114.

Lawrence, K.T., Herbert, T.D., Brown, C.M., Raymo, M.E., Haywood, A.M., 2009. High-amplitude variations in North Atlantic sea surface temperature during the early Pliocene warm period. Paleoceanography 24.

Lawrence, K.T., Liu, Z., Herbert, T.D., 2006. Evolution of the Eastern Tropical Pacific Through Plio-Pleistocene Glaciation. Science 312, 79-83.

Lisiecki, L.E., Raymo, M.E., 2005. A Pliocene-Pleistocene stack of 57 globally distributed benthic delta O-18 records. Paleoceanography 20, PA1003.

Liu, Z., Altabet, M.A., Herbert, T.D., 2008. Plio-Pleistocene denitrification in the eastern tropical North Pacific: Intensification at 2.1 Ma. Geochemistry, Geophysics, Geosystems 9, Q11006.

Liu, Z.H., Herbert, T.D., 2004. High-latitude influence on the eastern equatorial Pacific climate in the early Pleistocene epoch. Nature 427, 720-723.

Lübbecke, J.F., Böning, C.W., Keenlyside, N.S., Xie, S.P., 2010. On the connection between Benguela and equatorial Atlantic Nios and the role of the South Atlantic Anticyclone. J. Geophys. Res., C: Oceans Atmos. 115, C09015.

Lunt, D.J., Valdes, P.J., Haywood, A., Rutt, I.C., 2008. Closure of the Panama Seaway during the Pliocene: implications for climate and Northern Hemisphere glaciation. Clim. Dyn. 30, 1-18.

560 Lutjeharms, J.R.E., Stockton, P.L., 1987. Kinematics of the upwelling front off the
561 southern Africa. South African Journal of Marine Science 5, 35-49.

562 Lutjeharms, J.R.E., Valentine, H.R., 1987. Water types and volumetric considerations of
563 the South-East Atlantic upwelling regime. South African Journal of Marine Science 5, 63-
564 71.

565 Marlow, J.R., 2001. Application of UK37' for Long-term (Pliocene-Pleistocene)
566 Palaeoclimate Reconstruction. Newcastle upon Tyne, Newcastle upon Tyne.

567 Marlow, J.R., Lange, C.B., Wefer, G., Rosell-Mele, A., 2000. Upwelling intensification as
568 part of the Pliocene-Pleistocene climate transition. Science 290, 2288-2291.

569 Martinez-Garcia, A., Rosell-Mele, A., Jaccard, S.L., Geibert, W., Sigman, D.M., Haug,
570 G.H., 2011. Southern Ocean dust-climate coupling over the past four million years. Nature
571 476, 312-315.

572 Martinez-Garcia, A., Rosell-Mele, A., McClymont, E.L., Gersonde, R., Haug, G.H., 2010.
573 Subpolar Link to the Emergence of the Modern Equatorial Pacific Cold Tongue. Science
574 328, 1550-1553.

575 McClymont, E.L., Rosell-Mele, A., Giraudeau, J., Pierre, C., Lloyd, J.M., 2005. Alkenone
576 and coccolith records of the mid-Pleistocene in the south-east Atlantic: Implications for the
577 index and South African climate. Quat. Sci. Rev. 24, 1559-1572.

McIntyre, A., Ruddiman, W.F., Karlin, K., Mix, A.C., 1989. Surface water response of the equatorial Atlantic Ocean to orbital forcing. Paleoceanography 4, 19-55.

Meeuwis, J.M., Lutjeharms, J.R.E., 1990. Surface Thermal-Characteristics of the Angola-Benguela Front. South African Journal of Marine Science-Suid-Afrikaanse Tydskrif Vir Seewetenskap 9, 261-279.

Meyers, P.A., 2001. Miocene–Pleistocene sedimentary record of carbon burial under the Benguela Current upwelling system, southwestern margin of Africa, in: Wefer, G., Berger, W.H., Richter, C. (Eds.), Proceedings of the Ocean Drilling Program, Scientific Results, 175, pp. 1–19 [Online]. Available from World Wide Web: <http://www-odp.tamu.edu/publications/175_SR/VOLUME/CHAPTERS/SR175_106.PDF>.

Mollenhauer, G., Schneider, R.R., Jennerjahn, T., Müller, P.J., Wefer, G., 2004. Organic carbon accumulation in the South Atlantic Ocean: its modern, mid-Holocene and last glacial distribution. Global and Planetary Change 40, 249-266.

Molnar, P., 2008. Closing of the Central American Seaway and the ice age: A critical review. Paleoceanography 23.

Mudelsee, M., Raymo, M.E., 2005. Slow dynamics of the Northern Hemisphere glaciation. Paleoceanography 20, PA4022.

Paillard, D., Labeyrie, L., Yiou, P., 1996. Macintosh Program performs time-series analysis. Eos Trans. AGU 77, 379-379.

Peeters, F.J.C., Acheson, R., Brummer, G.-J.A., de Ruijter, W.P.M., Schneider, R.R., Ganssen, G.M., Ufkes, E., Kroon, D., 2004. Vigorous exchange between the Indian and Atlantic oceans at the end of the past five glacial periods. Nature 430, 661-665.

Philander, S.G., Fedorov, A.V., 2003. Role of tropics in changing the response to Milankovich forcing some three million years ago. Paleoceanography 18, Artn 1045.

Prange, M., Schulz, M., 2004. A coastal upwelling seesaw in the Atlantic Ocean as a result of the closure of the Central American Seaway. Geophys. Res. Lett. 31, L17207.

Ravelo, A.C., Andreasen, D.H., Lyle, M., Lyle, A.O., Wara, M.W., 2004. Regional climate shifts caused by gradual global cooling in the Pliocene epoch. Nature 429, 263-267.

Richter, I., Behera, S.K., Masumoto, Y., Taguchi, B., Komori, N., Yamagata, T., 2010. On the triggering of Benguela Niños: Remote equatorial versus local influences. Geophys. Res. Lett. 37, L20604.

Robinson, R.S., Meyers, P.A., 2002. Biogeochemical changes within the Benguela Current upwelling system during the Matuyama Diatom Maximum: Nitrogen isotope evidence from Ocean Drilling Program Sites 1082 and 1084. Paleoceanography 17.

Rogers, J., Bremner, J.M., 1991. The Benguela ecosystem, Part VII: Marine geological aspects. Marine Biology Annual Review 29, 1-85.

Rouault, M., Florenchie, P., Fauchereau, N., Reason, C.J.C., 2003. South East tropical Atlantic warm events and southern African rainfall. Geophys. Res. Lett. 30, 9.1 - 9.4.

Schneider, R.R., Müller, P.J., 1995. What Role Has Upwelling Played in the Global Carbon and Climatic Cycles on a Million-Year Time Scale?, in: Summerhayes, C.P., Emeis, K.-C., Angel, M.V., Smith, R.L., Zeitschel, B. (Eds.), Upwelling in the Ocean: Modern Processes and Ancient Records. John Wiley, pp. 361-380.

Shannon, L.V., Boyd, A.J., Brundrit, G.B., Tauntonclark, J., 1986. On the Existence of an El-Nino-Type Phenomenon in the Benguela System. J. Mar. Res. 44, 495-520.

Siesser, W.G., 1980. Late Miocene origin of the Benguela upswelling system off Northern Namibia. Science 208, 283-285.

Sigman, D.M., Jaccard, S.L., Haug, G.H., 2004. Polar ocean stratification in a cold climate. Nature 428(6978), 59-63.

Summerhayes, C.P., Kroon, D., Rosell-Mele, A., Jordan, R.W., Schrader, H.J., Hearn, R., Villanueva, J., Grimali, J.O., Eglinton, G., 1995. Variability in the Benguela Current upwelling system over the past 70,000 years. Progress in Oceanography 35, 207-251.

Tiedemann, T., 1991. Acht Millionen Jahre Klimageschichte von Nordwest Afrika und Palao-Ozeanographie des angrenzenden Atlanktis: hochauflosende Zeitreihen von ODP-Sites 658–661, Berichte-Reports, Geol.-Palaontologisches Institut. Univ. Kiel, Kiel, p. 190.

Wefer, G., Berger, W.H., Richter, C., et_al., 1998. Proc. ODP, Init. Repts., 175. Ocean Drilling Program, College Station, TX.

Figure 1. Location of the records discussed in the text. Modern annual mean sea surface temperature values are from the World Ocean Atlas 2009. Black arrows are schematic representation of the main currents relevant for the discussion in the text (LC: Leeuwin Current, ITF: Indonesian Throughflow, AGC: Agulhas Current, SAC: South Atlantic Current, BCC: Benguela Costal Current, BOC: Benguela Oceanic Current, AC: Angola Current, ABFZ: Angola-Benguela Frontal Zone).

Figure 2. Comparison of the alkenone sea surface temperature (SST) reconstructions in the Benguela region after graphical alignment. (A) SST at ODP site 1084 (green line) and ODP Site 1082 (black line) (Etourneau et al., 2009). (B) SST at ODP site 1081 (red line) and ODP Site 1082.

Figure 3. Age/depth pointers obtained after aligning the alkenones SST records of ODP sites 1084 and 1081 to the SST reconstruction form ODP Site 1082 (Etourneau et al., 2009) (red dots), compared to those obtained by magnetostratigraphy and calcareous nannofossil biostratigraphy (Wefer et al., 1998).

Figure 4. Evolution of the Benguela upwelling system over the past 5Ma. (A) Lisiecki and Raymo global benthic $\delta^{18}O$ stack (Lisiecki and Raymo, 2005). (B) Sea surface temperature evolution of the Benguela region at ODP Site 1084 (green line), ODP Site 1082 (black line) (Etourneau et al., 2009) and ODP Site 1081 (red line). Thick lines represent 600ky running averages. (C) Export production changes in the Benguela upwelling system over the last 5

Ma inferred from alkenone mass accumulation rates (MAR) at ODP Site 1084 (green line), ODP Site 1082 (black line) (Etourneau et al., 2009) and ODP Site 1081 (red line). (D) Evolution of the latitudinal gradient between ODP Sites 1082/1081 and ODP Site 1084 calculated by subtracting the thick lines in panel B, and long-term trend of dust/Fe deposition in the Southern Ocean (Martinez-Garcia et al., 2011) calculated using a 600ky running average.

Figure 5. Evolution of the Indonesian Throughflow and the Southern Ocean at the end of the Pliocene Benguela "El Niño"-like conditions. (A) Lisiecki and Raymo global benthic $\delta^{18}O$ stack (Lisiecki and Raymo, 2005). (B) Sea surface temperature evolution of the Benguela region at ODP Site 1084 (green line), and ODP Site 1081 (red line). (C) Mg/Ca *Globorotalia crassaformis* subsurface temperature estimates from DSDP Site 214 (Karas et al., 2009). (D) Alkenone-based reconstruction of Southern Ocean SST at ODP Site 1090 (Martinez-Garcia et al., 2010).

Figure 6. Continuous wavelet power spectrum of (A) Sea Surface Temperature (SST) at ODP Site 1082 (Etourneau et al., 2009) and (B) ODP Site 1084, Alkenones MAR at (C) ODP Site 1082 (Etourneau et al., 2009) and (D) ODP Site 1084, and (E) Lisiecki and Raymo (LR04) benthic d18O stack (Lisiecki and Raymo, 2005), calculated using the methods proposed by Grinsted et al. (Grinsted et al., 2004). All the series were detrended and interpolated to 4 ky before the spectral analysis. The thick black contour designates the 5% significance level against red noise. The cone of influence (COI) where edge effects might become significant is shown as a lighter shade.

Figure 7. Continuous wavelet power spectrum of (A) Lisiecki and Raymo (LR04) benthic $\delta^{18}O$ stack (Lisiecki and Raymo, 2005), (B) Sea Surface Temperature (SST) in the Benguela current (ODP Site 1082) (Etourneau et al., 2009), and (C) SST in the Eastern Equatorial Pacific (ODP Site 846) (Lawrence et al., 2006), calculated using the methods proposed by Grinsted et al. (Grinsted et al., 2004). All the series were detrended and interpolated to 4ky before the spectral analysis. The thick black contour designates the 5% significance level against red noise. The cone of influence (COI) where edge effects might become significant is shown as a lighter shade.

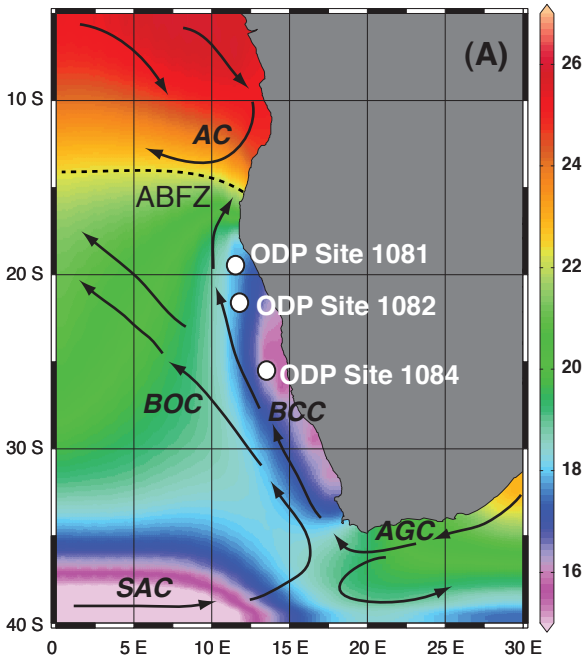
(A)
AC
ABFZ
ODP Site 1081
ODP Site 1082
ODP Site 1084
BOC
BCC
AGC
SAC
10 S
20 S
30 S
40 S
0
5 E
10 E
15 E
20 E
25 E
30 E
26
24
22
20
18
16

Fig. 1

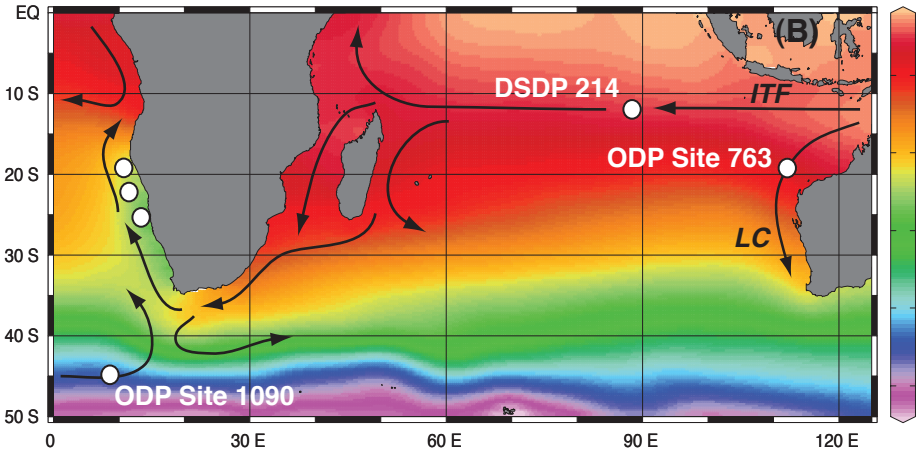
(B)
DSDP 214
ITF
ODP Site 763
LC
ODP Site 1090
EQ
10 S
20 S
30 S
40 S
50 S
0
30 E
60 E
90 E
120 E
25
20
15
10
5

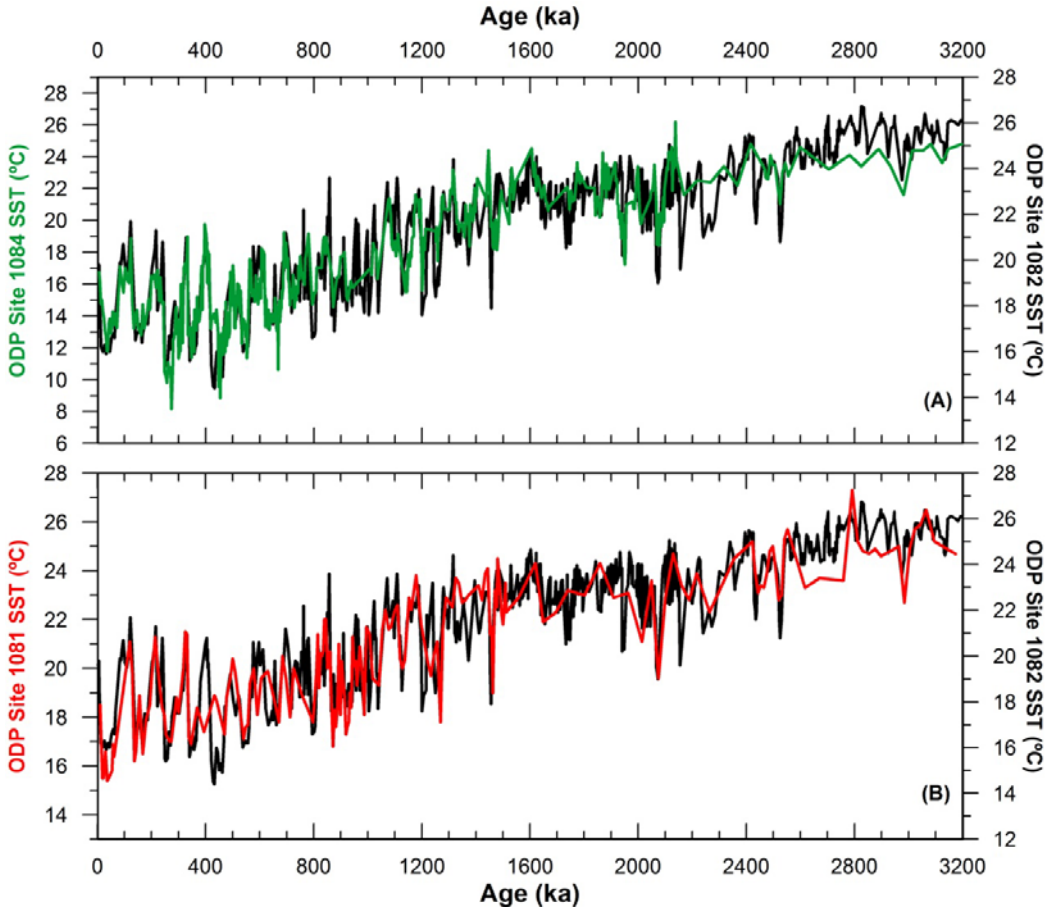
Age (ka)
0
400
800
1200
1600
2000
2400
2800
3200
ODP Site 1084 SST (°C)
ODP Site 1082 SST (°C)
(A)
ODP Site 1081 SST (°C)
ODP Site 1082 SST (°C)
(B)
Age (ka)

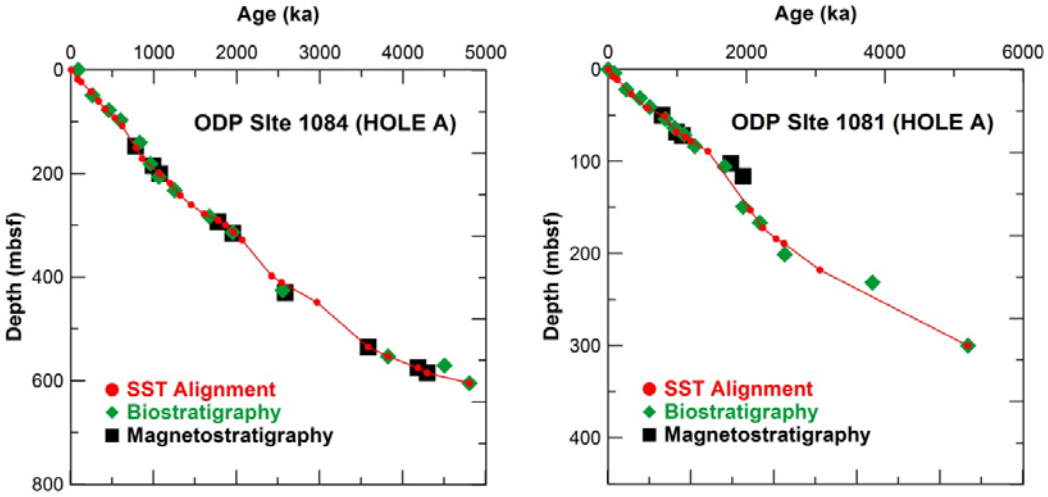
Age (ka)
0
1000
2000
3000
4000
5000
Depth (mbsf)
0
200
400
600
800
ODP SIte 1084 (HOLE A)
SST Alignment
Biostratigraphy
Magnetostratigraphy
Age (ka)
0
2000
4000
6000
Depth (mbsf)
0
100
200
300
400
ODP SIte 1081 (HOLE A)
SST Alignment
Biostratigraphy
Magnetostratigraphy

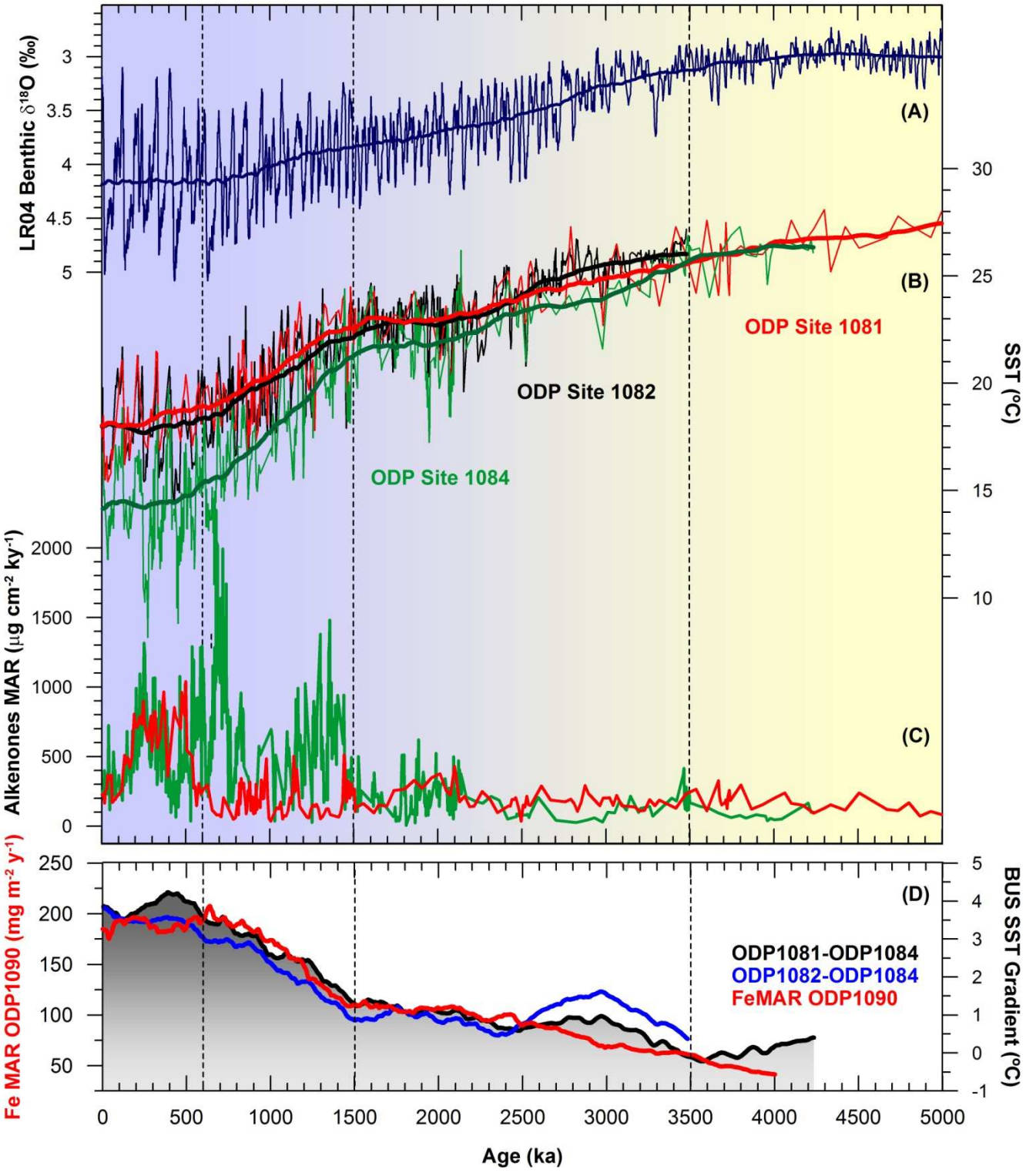
LR04 Benthic δ18O (‰)
3
3.5
4
4.5
5
(A)
30
25
20
15
10
SST (°C)
(B)
ODP Site 1081
ODP Site 1082
ODP Site 1084
Alkenones MAR (μg cm-2 ky-1)
2000
1500
1000
500
0
(C)
Fe MAR ODP1090 (mg m-2 y-1)
250
200
150
100
50
(D)
ODP1081-ODP1084
ODP1082-ODP1084
FeMAR ODP1090
5
4
3
2
1
0
-1
BUS SST Gradient (°C)
0
500
1000
1500
2000
2500
3000
3500
4000
4500
5000
Age (ka)

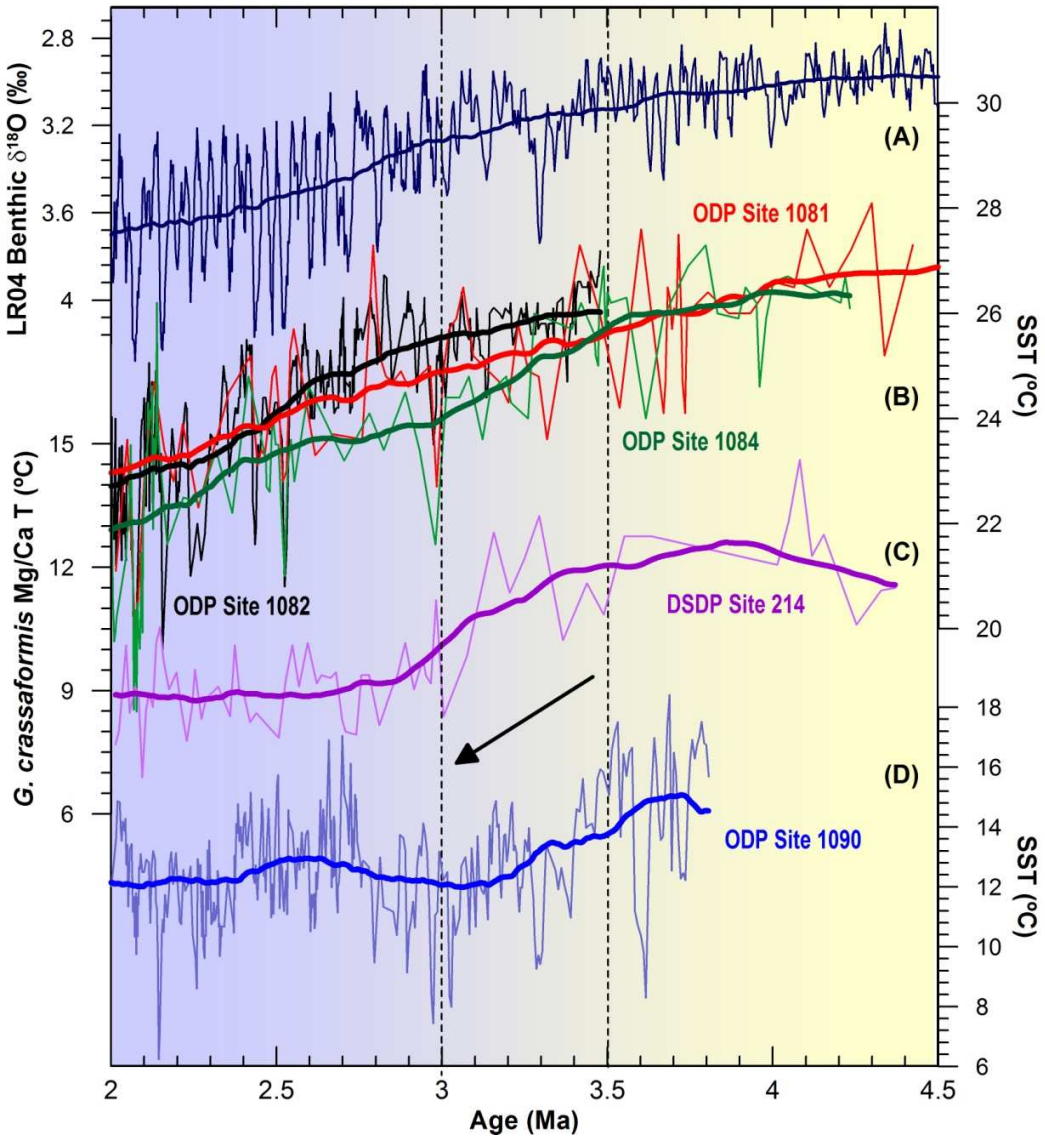
LR04 Benthic δ18O (‰)
G. crassaformis Mg/Ca T (°C)
SST (°C)
SST (°C)
Age (Ma)
(A)
(B)
(C)
(D)
ODP Site 1081
ODP Site 1084
ODP Site 1082
DSDP Site 214
ODP Site 1090

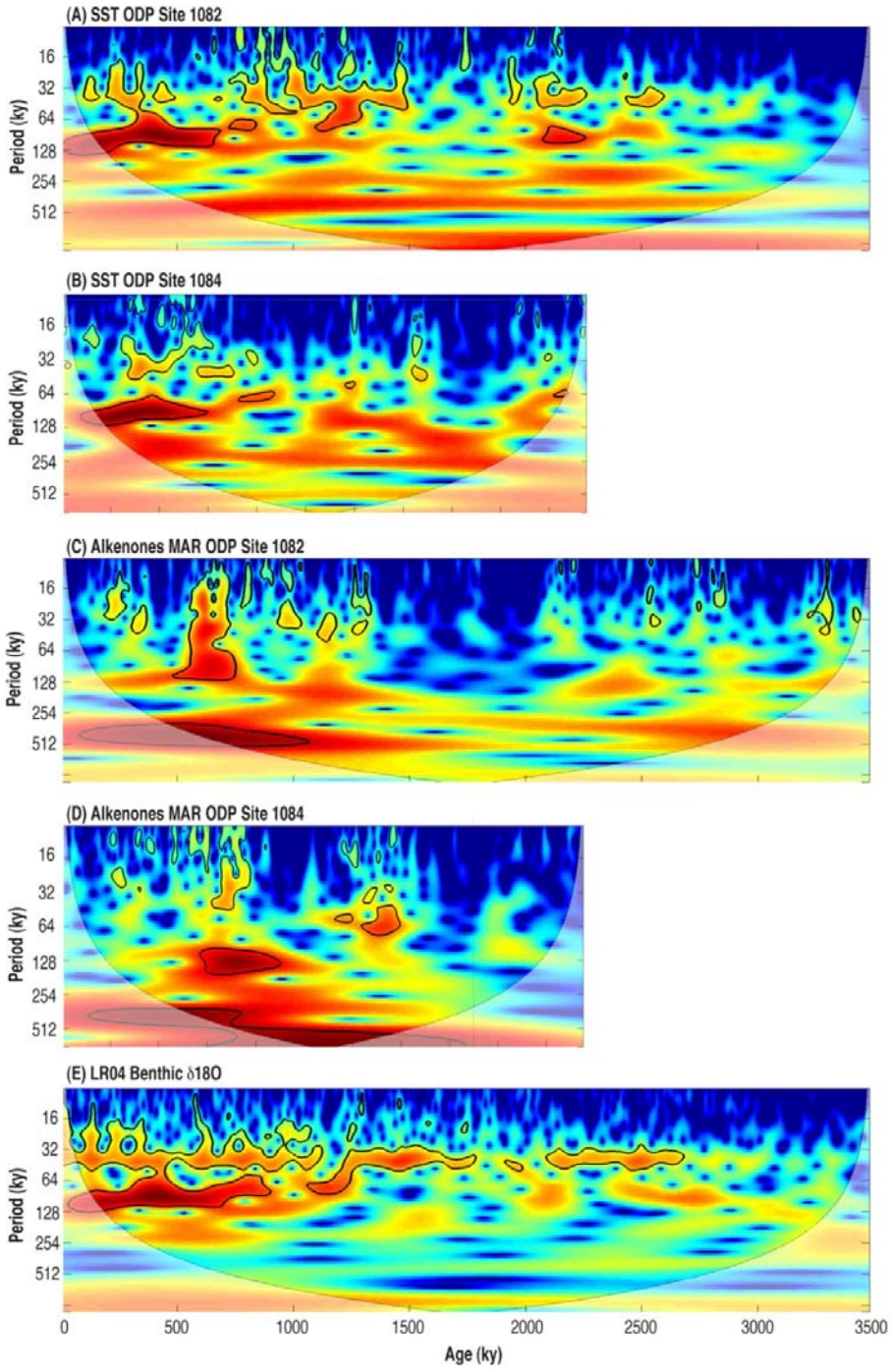
(A) SST ODP Site 1082
(B) SST ODP Site 1084
(C) Alkenones MAR ODP Site 1082
(D) Alkenones MAR ODP Site 1084
(E) LR04 Benthic δ18O
Period (ky)
16
32
64
128
254
512
0
500
1000
1500
2000
2500
3000
3500
Age (ky)

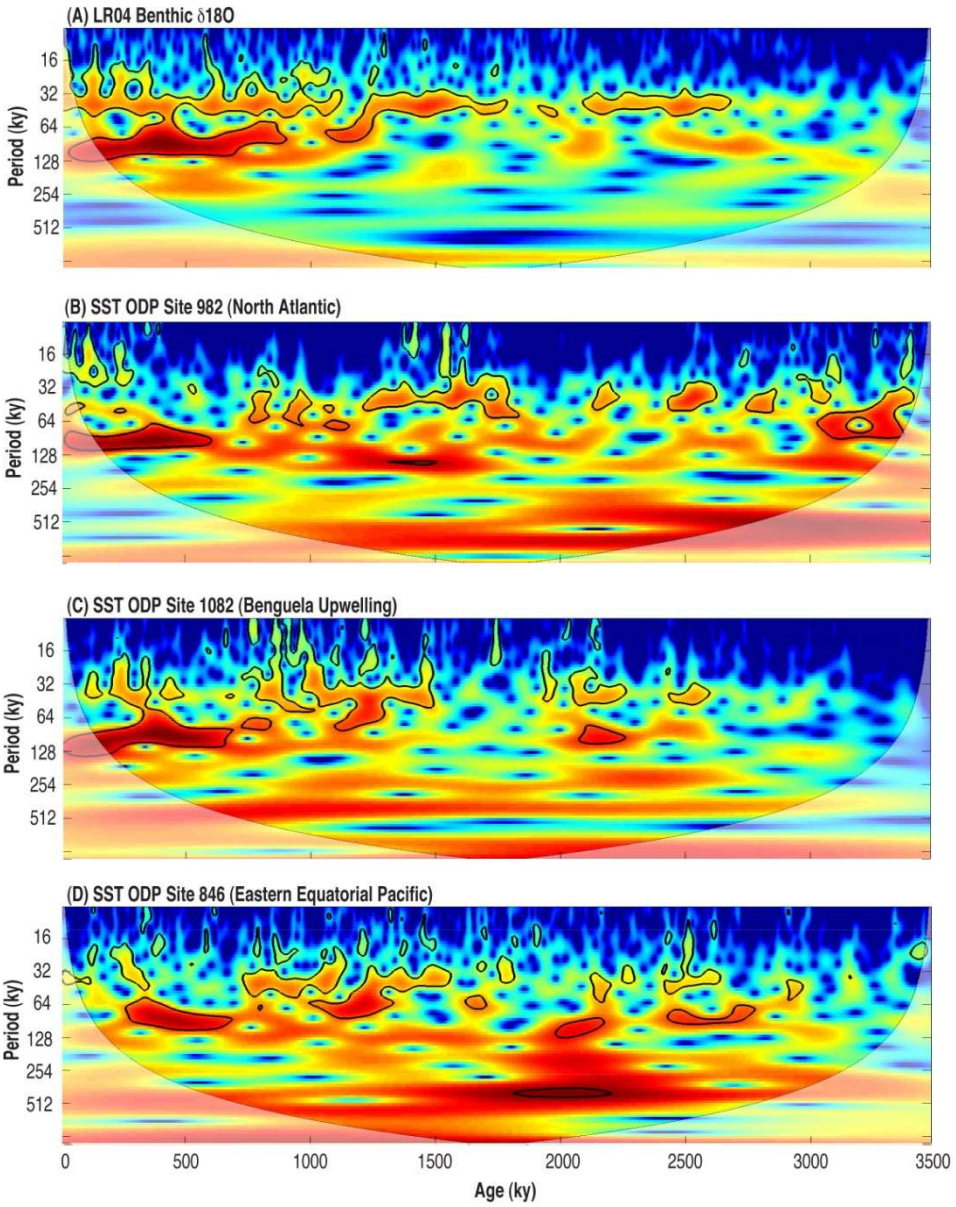
(A) LR04 Benthic δ18O
(B) SST ODP Site 982 (North Atlantic)
(C) SST ODP Site 1082 (Benguela Upwelling)
(D) SST ODP Site 846 (Eastern Equatorial Pacific)
Period (ky)
16
32
64
128
254
512
0
500
1000
1500
2000
2500
3000
3500
Age (ky)